Available online at www.sciencedirect.com
ScienceDirect
Journal of the European Ceramic Society 28 (2008) 2567–2572
www.elsevier.com/locate/jeurceramsoc

An in situ study of the formation of multiferroic bismuth ferrite using high resolution synchrotron X-ray powder diffraction

M. Thrall [a], R. Freer [a], C. Martin [a], F. Azough [a], B. Patterson [b], R.J. Cernik [a,*]

[a] *Materials Science Centre, School of Materials, University of Manchester, Grosvenor Street, Manchester M1 7HS, UK*
[b] *Swiss Light Source, Paul Scherrer Institut, 5232 Villigen PSI, Switzerland*

Received 15 January 2008; received in revised form 28 March 2008; accepted 30 March 2008
Available online 22 May 2008

Abstract

The synthesis of multiferroic $BiFeO_3$ has been undertaken in situ using both vacuum and argon atmospheres. We have collected and refined synchrotron X-ray powder diffraction data from pressed pellets of the starting powders of Bi_2O_3 and Fe_2O_3 at intervals in the reaction to form the final multiferroic $BiFeO_3$ product. Data were collected at 3-min intervals following as realistically as possible the sintering regimes used in industry. The difference in the transformation temperature of monoclinic Bi_2O_3 to cubic Bi_2O_3 was found to be 650 and 700 °C when samples were sintered in a vacuum and argon environments, respectively. It was found that this reaction was 75% complete before the multiferroic product began to form. In both cases it was found that the quantity of Fe_2O_3 was unaffected by increasing temperature until after the transition of monoclinic to cubic Bi_2O_3 had reached its maximum value. After this transition the quantities of cubic Bi_2O_3 and Fe_2O_3 were found to decrease at very similar rates yielding the final $BiFeO_3$ structure. An SEM study of the bulk microstructure of the $BiFeO_3$ product showed a poor densification due to incomplete reactions between the remaining Bi_2O_3 and Fe_2O_3.
© 2008 Elsevier Ltd. All rights reserved.

Keywords: Multiferroic; Bismuth ferrite; Synchrotron powder diffraction

1. Introduction

Multiferroics are materials which exhibit the simultaneous presence of ferromagnetic, ferroelectric and ferroelastic coupled order parameters within a single phase[1] (or at least two of these characteristics). The perovskite $BiFeO_3$ has been found to be multiferroic, having ferroelectric ordering below the Curie transition temperature $T_c \sim 830$ °C and a G type antiferromagnetic transition at $T_n \sim 370$ °C.[2] Extensive neutron and X-ray diffraction studies have shown $BiFeO_3$ to crystallise in a rhombohedral distorted perovskite cell, with space group *R*3*c* and unit cell parameters $a = 5.616$ Å and α 59.35°.[3,4]

Pradham et al.[2] and Wang et al.[5] reported that it is difficult to obtain single phase $BiFeO_3$ in the form of bulk sintered samples by conventional mixed oxide sintering due to the formation of impurity phases such as $Bi_2Fe_4O_9$ and $Bi_{12}(Bi_{0.5}Fe_{0.5})O_{19.5}$. Attempts to remove these secondary phases have included leaching out impurity phases with nitric acid[6] as well as use of rapid liquid sintering techniques where samples were subjected to heating and cooling rates of the order of 100° s^{-1}.[2,5,7] In addition, high levels of electrical conductivity have been detected in sintered $BiFeO_3$ samples giving poor saturation in ferroelectric hysteresis loops.[2] It has been suggested that reason for these high levels of conductivity is the existence of multiple valence states of the Fe ion, resulting from the presence of oxygen vacancies created throughout the sintering process.[2,5] However, X-ray photoelectron spectroscopy (XPS) measurements by Wang et al.[5] have provided evidence that only Fe^{3+} is present.

Attempts to reduce electrical losses and improve the saturation of ferroelectric hysteresis loops have included dispersing $BiFeO_3$ within highly resistive perovskites such as $BaTiO_3$, $PbTiO_3$ and $SrTiO_3$.[6,8–10] Electrical measurements of these samples indicated slight reductions in dielectric loss but no significant change in the poorly saturated ferroelectric hysteresis loops.

In order to optimise the synthesis and sintering process to produce a more stable product we have studied the formation of $BiFeO_3$ from the starting oxides Bi_2O_3 and Fe_2O_3 through to the final multiferroic product in both vacuum and argon environments. In situ synchrotron radiation X-ray diffraction (SR-XRD)

* Corresponding author.
E-mail address: r.cernik@manchester.ac.uk (R.J. Cernik).

0955-2219/$ – see front matter © 2008 Elsevier Ltd. All rights reserved.
doi:10.1016/j.jeurceramsoc.2008.03.029

measurements and Scanning Electron microscopy were used to characterise the final product.

2. Experimental procedure

2.1. Sample preparation

The starting powders of Bi_2O_3 (≥98% purity) and Fe_2O_3 (≥99% purity) were mixed (1:1 ratio Bi_2O_3:Fe_2O_3) with propan-2-ol and zirconia media in a polyurethane flask by a process of vibro-milling for 16 h. The powder was then dried at 100 °C for 4 h to ensure complete removal of organic species. After drying, 2 g batches of the mixed oxide powder were compacted in a steel die at a load of 10 kg/cm^2 yielding cylindrical samples 10 mm diameter and 4 mm thick.

2.2. Synchrotron in situ powder diffraction

The in situ synchrotron powder diffraction analyses for the sintering cycle of $BiFeO_3$ were undertaken on the X04SA and 6.2 Materials Science beam lines[11–13] located at the Swiss Light Source (SLS) and the Daresbury Laboratory Synchrotron Radiation Source (SRS) respectively. The use of curved linear position sensitive photon counting detectors was necessary to measure a refineable range of the powder diffraction pattern at a suitable rate during the reaction. The rapid data acquisition system at Daresbury is a modification of that already described for station 16.3.[14] The time resolved XRD data sets were collected at approximately 3-min intervals during the sintering process. The RAPID2[15] detector used on beam line 6.2 is a gas filled wire chamber where the position of the incident X-ray photon is measured by gas amplification and interpolated by a series of uniformly spaced anode wires. The Mythen I[16] detector used on the X04SA beam line is based on a silicon microstrip detector with a 50-μm pitch. The detector has a basic level pulse height discriminator but no real energy resolution. The Mythen I detector has an inherently higher spatial resolution (0.004°) than RAPID2 (0.06°) but has a lower count rate. The lower count rate was limited to 3 kHz by random electronic events. It was found, during the course of this experiment, that the spatial stability of Mythen I was superior to that of RAPID2 and enabled more accurate Rietveld refinements to be undertaken. However, both detectors yielded usable data. Mythen I gave a number of random counts in channels following high count rates. These defects were corrected by collecting six data sets and coincidence matching in order to remove the random counts. In addition Mythen I was operated at two angles, separated by one degree, in order to cover the dead regions between strips. The next generation of strip detectors from the SLS (Mythen II) has corrected the random count problem.[17] One data set collected from Mythen I was therefore the sum of 12 data sets, half of which were collected 1° higher in 2θ. No such correction was necessary with the RAPID2 system yielding a faster duty cycle performance than Mythen I. Both the data from Mythen I and RAPID2 allowed a full Rietveld refinement of the evolving structures during the processing cycle.

On both systems the pressed samples were heated using a tantalum foil furnace enclosing the sample on three sides.[18] In order to prevent oxidation of the tantalum heating foil the sintering environment was (i) a vacuum of 10^{-4} mbar (SLS) and (ii) flowing argon gas (SRS, Daresbury). The latter case more closely resembled conventional sintering conditions. In both experiments an S-type thermocouple was positioned in close proximity, (∼1 mm) above the top surface of the sample, to obtain temperature control of ±1 °C relative to the sample surface during sintering.[18] The furnace temperature was raised at a rate of 3 °C min^{-1} to a maximum temperature of 920 °C. XRD spectra were taken continuously throughout the heating of the sample. The collection time for each spectrum was 3 min therefore the data has an inherent uncertainty of ±4.5° about each measured temperature. An additional constant omega oscillation of ±1.5° was applied to the inner rotary stage of the X04SA powder diffraction beam line[11] to create increased randomisation of grain orientation for better counting statistics.

The X-ray powder diffraction patterns were refined with the software program TOPAS using multi-pattern Rietveld quantitative analysis.[19,20] The resulting lattice parameters, phase percentages and crystal sizes were determined as a function of rising temperature.

2.3. Scanning electron microscopy

For comparison purposes a series of samples were also sintered in a conventional tube furnace in an argon atmosphere using the same heating regime as the samples sintered on the synchrotron beam lines. All samples were cut, ground on 1200 grade SiC and polished down to 0.5 μm diamond paste and carbon coated using an Edwards E306A carbon evaporator. Scanning electron microscopy was undertaken using a Phillips XL30 field emission gun (FEG). Images were collected from both the ground and polished and as sintered surfaces.

3. Results

3.1. Sintering $BiFeO_3$ in vacuum

Fig. 1 shows seven XRD patterns taken at critical stages during the sintering of a pressed pellet under vacuum. The initial ambient temperature XRD spectrum shows the expected phases; monoclinic P21/c Bi_2O_3 and trigonal R-3C Fe_2O_3. As the temperature was increased to 400 °C the cell parameters for Bi_2O_3 and Fe_2O_3 increased, highlighted by the separation of the (2 1 0) and (2 1 2) peaks, circled in Fig. 1. Above 500 °C the low temperature monoclinic phase of Bi_2O_3 transformed into a cubic phase with space group *I*23. There was a 75% transformation of the Bi_2O_3 monoclinic to cubic phase by 650 °C. This temperature coincided with the first appearance of significant quantities of the final multiferroic $BiFeO_3$ phase. This was most apparent at 2θ values of 21° and 22° where the (2 1 1) and (0 1 1) peaks, characteristic of $BiFeO_3$, began to form. At temperatures above 650 °C these peaks were seen to grow rapidly signifying advanced crystallisation of the $BiFeO_3$ structure.

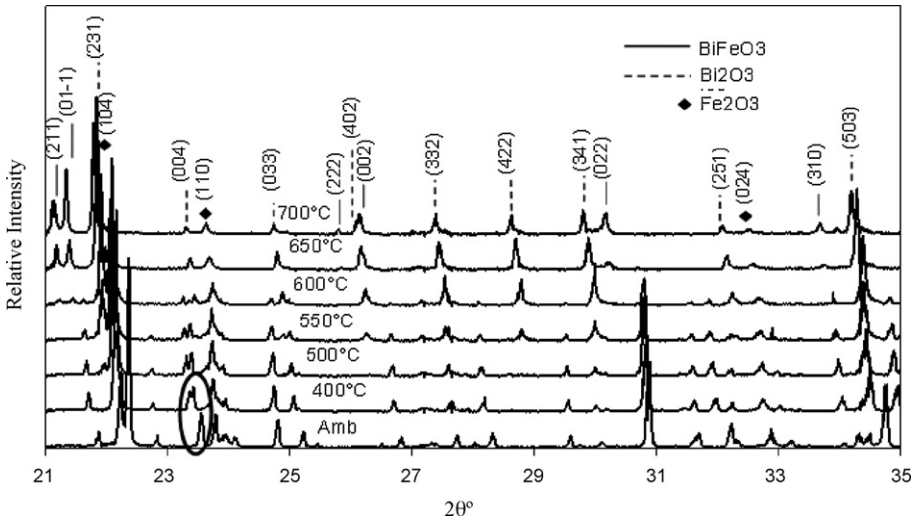

Fig. 1. Selected powder diffraction patterns collected during the synthesis of multiferroic $BiFeO_3$ in a vacuum environment on the X04SA powder diffraction beam line.

Each data set collected in a vacuum environment at the Swiss Light Source yielded, after refinement a quantified phase percentage accurate to ±2%. These results are shown in Fig. 2 as a function of temperature. This analysis reveals a transformation of Bi_2O_3 from $P21/c$ to $I23$ between 500 and 650 °C. The trigonal R-3C structure of Fe_2O_3 did not react to form the final bismuth ferrite product until 650 °C where the transformation to the cubic form of Bi_2O_3 was well advanced. The onset of changes in the amount of Fe_2O_3 coincided with the maximum of Bi_2O_3 transformed to the cubic phase as well as the beginnings of a rapid increase in the crystallisation of the rhombohedral $R3c$ $BiFeO_3$ phase. These results suggest that the optimum conditions for the synthesis of $BiFeO_3$ are strongly dependant on the conversion of the monoclinic Bi_2O_3 to the cubic phase.

At the maximum sintering temperature of 700 °C the $BiFeO_3$ lattice parameters were found to be: $a = b = c = 5.7$ Å and $\alpha = \beta = \gamma = 59.37°$. Experimental limits on the furnace during this experiment restricted the maximum temperature to 700 °C and prevented a full examination of the final multiferroic product.

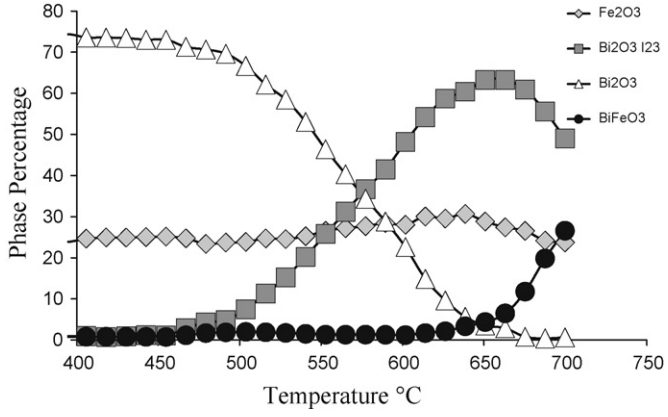

Fig. 2. Quantified phase percentages obtained from full pattern Rietveld refinement of multiple data sets during the synthesis of $BiFeO_3$ in a vacuum. Transformation from the monoclinic low temperature form of Bi_2O_3 to the high temperature cubic phase was observed before the $BiFeO_3$ structure began to form. The size of the point markers represent the uncertainty in both axes.

Fig. 3 shows the lattice parameters for Fe_2O_3 and Bi_2O_3, there is a small but steady increase with temperature for both the monoclinic Bi_2O_3 and trigonal Fe_2O_3 as expected. Fig. 3a and b shows that between 600 and 650 °C there is an increase in gradient of the lattice parameters with respect to temperature in all cases. These observations correlate well with the reactions occurring between cubic Bi_2O_3 and Fe_2O_3 phases mentioned earlier. This suggests that the reactions leading to the formation of the final multiferoic $BiFeO_3$ are initiated between 600 and 650 °C.

3.2. *Sintering $BiFeO_3$ in a argon environment*

The synthesis of $BiFeO_3$ was repeated using a sintering atmosphere of argon. A similar sintering profile was observed and the phase percentages are shown in Fig. 4. However, the onset of all the observed reactions occurred at higher temperatures compared to those for samples sintered in vacuum. The transformation between the monoclinic and cubic phases of Bi_2O_3 occurred 50 °C higher than previously found in vacuum. The reactions between the high temperature cubic Bi_2O_3 and Fe_2O_3 producing the final multiferroic product $BiFeO_3$ were found to occur between 800 and 850 °C.

On the basis of differential scanning calorimetry Pradham[2] noted a key reaction within the mixed oxide sample at 820 °C. This was attributed to a change in the Bi_2O_3 structure from the initial monoclinic phase to a high temperature cubic phase. However, in light of the present study it would appear that cubic phase formation occurs at lower temperature, and that the reaction observed by Pradham[2] was instead related to the reactions between the cubic Bi_2O_3 and Fe_2O_3 phases.

At approximately 830 °C the $BiFeO_3$ phase reaches a maximum value of 75 ± 2%. Above this temperature a breakdown of $BiFeO_3$ was observed resulting in an increase in the Fe_2O_3 phase as well as the formation of a new orthorhombic $Bi_2Fe_4O_9$

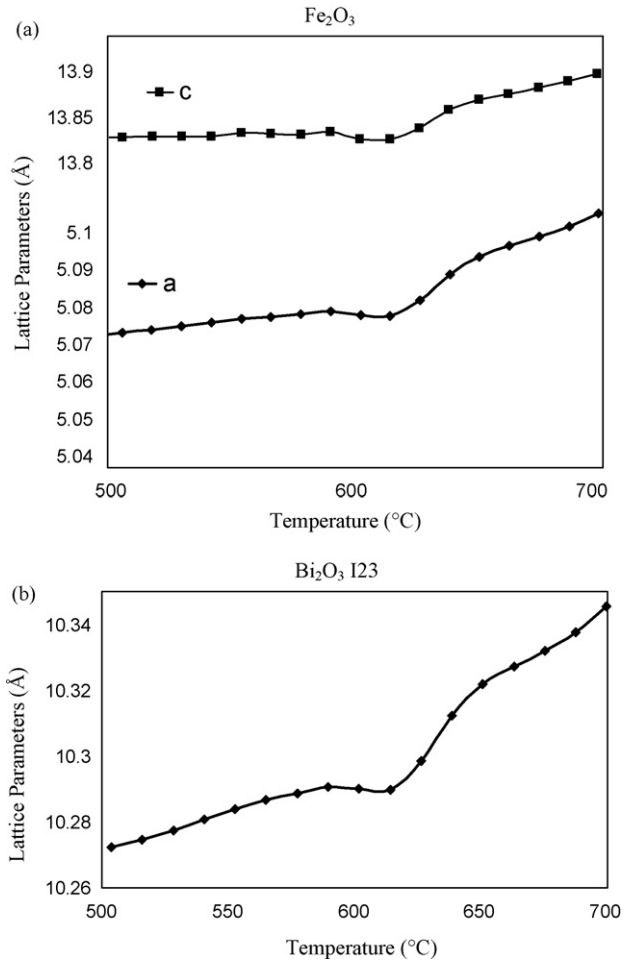

Fig. 3. The lattice parameter refinements for Fe_2O_3 show a clear structural change between 600 and 650 °C indicating the reaction between the mixed oxides (a). A very similar effect was observed from the lattice parameter refinements for the cubic I23 Bi_2O_3 phase (b).

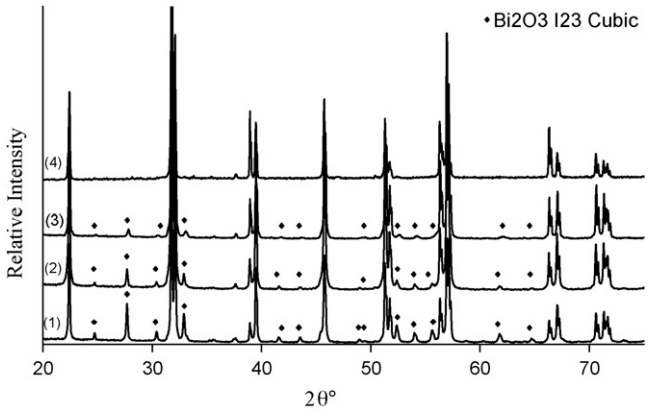

Fig. 5. XRD spectra taken of the sintered bulk and surface of $BiFeO_3$ samples sintered using the rapid liquid sintering (1) 850 °C bulk surface, (2) 850 °C sintered surface, (3) 880 °C bulk surface, and (4) 880 °C sintered surface. The markers show the positions of the Bi_2O_3 cubic phase.

phase. At temperatures above 830 °C the new phase was seen to continue growing at the expense of the $BiFeO_3$ phase.

3.3. Activation energy

A small range of the phase percentage curves was selected for further study. These are shown in Figs. 2 and 4 coinciding with the onset of the development of the $BiFeO_3$ phase up to its maximum value. The activation energy of the formation $BiFeO_3$ was calculated from a simple Arrhenius model shown in Fig. 6. The values of 3.98 and 2.49 eV for the reactions occurring in argon and vacuum environments show higher activation energy in the argon environment. This has been attributed to the volatility of reactant species giving rise to greater bulk mobility.

3.4. Rapid liquid sintering

Following the in situ synchrotron experiments further investigations were conducted into the sintering process of bulk phase

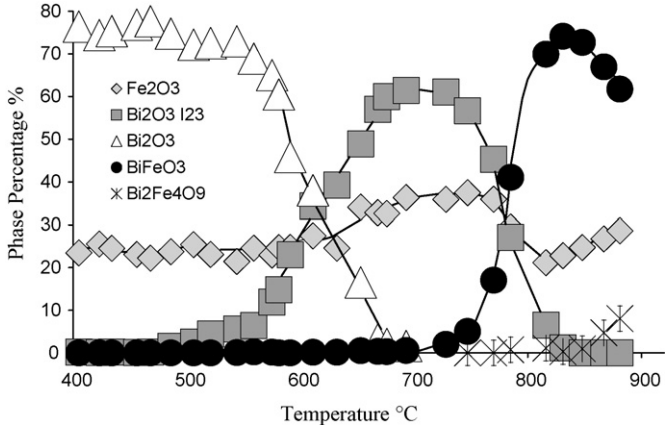

Fig. 4. The phase percentages obtained from quantitative Rietveld refinement of multiple data sets during the sintering of $BiFeO_3$ in argon. The phase transformation profile is similar to that observed when sintering $BiFeO_3$ in a vacuum but reactions occur at higher temperatures. The size of the point markers represent the uncertainty in both axes.

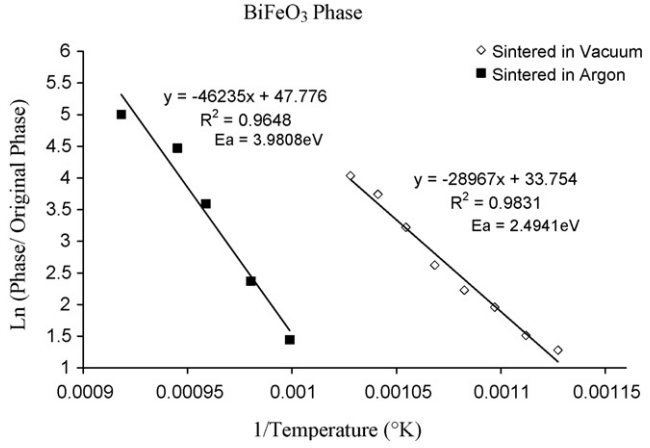

Fig. 6. A simple Arrhenius model for the formation of the $BiFeO_3$ cubic phase when the sample is sintered in vacuum and argon environments. The activation energy values, E_a show that more energy is required to complete the same reaction when sintering in argon than in a vacuum.

$BiFeO_3$ with the application of rapid liquid phase sintering described in the studies of Pradham et al.[2] and Wang et al.[5] Samples were heated at a rate of 100 °C s^{-1} to temperatures of 850 and 880 °C and then held at maximum temperature for 7.5 min to 10 h before being quenched. X-ray diffraction measurements taken using a standard Cu Kα XRD source showed that the samples sintered at 850 °C had formed an additional secondary high temperature Bi_2O_3 cubic phase and some remaining unreacted Fe_2O_3 (Fig. 5). The diffraction peaks associated with this phase were seen in both spectra from the bulk and sintered surfaces but was much more pronounced in the bulk sample with Rietveld refinement confirming a quantified phase percentage of 16% ± 2%. In contrast, the sample sintered at 880 °C contained no detectable Bi_2O_3 cubic phase on the sintered surface, but did, however, have 5% Bi_2O_3 cubic phase present within the bulk of the sample (Fig. 5). Increasing the time spent at the maximum sintering temperature of 880 °C from the prescribed 7.5–30 min led to a slight reduction of the Bi_2O_3 cubic phase within the bulk sample. However, if the time spent at the maximum sintering temperature was increased to more than 4 h, formation of the orthorhombic $Bi_2Fe_4O_9$ phase began. Increasing the time spent at maximum sintering temperature to 6 and 10 h caused complete conversion from the multiferroic $BiFeO_3$ to $Bi_2Fe_4O_9$. Similar changes were found if the maximum sintering temperature was increased above 880 °C.

Comparisons of weight loss between the initial mixed oxide pressed cylinders and final sintered products gave a weight loss reduction of 7.2% when samples were sintered at 880 °C for 7.5 min (Fig. 6). Increasing sintering time to longer periods between 6 and 10 h the corresponding weight loss was 27 and 32%, respectively. As suggested by Pradham[2] this weight loss is due to increased boil off of the bismuth which acts to alter the 1:1 ratio of Bi_2O_3 and Fe_2O_3. This is because less bismuth is available to create the higher ion content phase hence the formation of the $Bi_2Fe_4O_9$ phase.

Fig. 7 shows an SEM taken from the polished surface of the $BiFeO_3$ sample sintered at 880 °C for 0.5 h. The measured grain size varied between 10 and 30 μm in length across the sample surface. The sample has a high level of porosity and low densification suggesting local material loss due to evaporation.

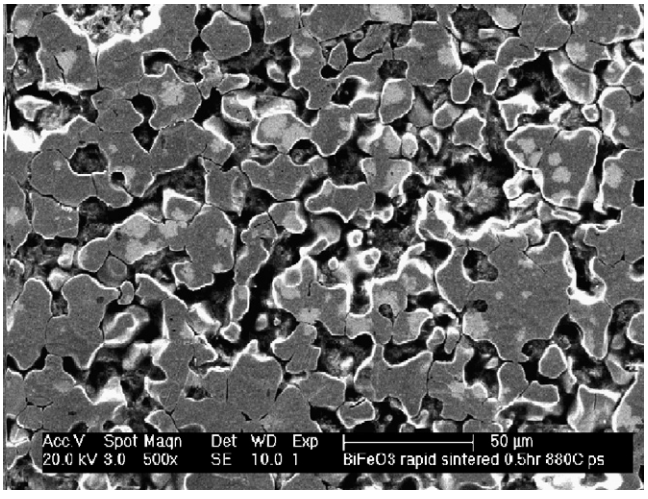

Fig. 7. SEM image taken of $BiFeO_3$ sintered at 880 °C for 0.5 h. Porous regions are seen to develop once the temperature is raised and held at 880 °C.

4. Conclusions

In conclusion the crystallisation of the mulitiferroic $BiFeO_3$ is dependant on the transformation of the Bi_2O_3 mixed oxide powder to the high temperature cubic phase. It is only after this transformation has occurred that a reaction can be seen between the Bi_2O_3 and Fe_2O_3 phases. These reactions were found to occur at higher temperatures when the samples were sintered in air and argon compared to a vacuum. Activation energies calculated for the Bi_2O_3 and Fe_2O_3 mixed oxides as well as the final $BiFeO_3$ phase have all confirmed higher activation energies when sintering in argon compared to vacuum. This explains the need for the higher sintering temperatures required for the formation of the $BiFeO_3$ phase in argon. We believe the reason for this is the very low gas pressure in the vacuum environment giving increased material transport and evaporation as the boil off temperature for each of the associated mixed oxides is reduced. By increasing the material transport within the bulk sample there would is more opportunity for the iron and bismuth to react producing the final multiferroic product $BiFeO_3$.

Large levels of porosity and poor sample densification have been shown in bulk sintered $BiFeO_3$ with incomplete reactions between the high temperature Bi_2O_3 phase and remaining Fe_2O_3. Low levels of densification can be related to high levels of electrical loss previously observed for $BiFeO_3$.[2,5,7] Furthermore if the maximum sintering temperature is raised higher than 880 °C or the sample is left to sinter for a longer time than 30 min, then the $BiFeO_3$ structure begins to break down and the new orthorhombic$Bi_2Fe_4O_9$ phase begins to form.

The use of rapid liquid phase sintering techniques described in Refs.[2,5,7] is useful in reducing secondary phase formation by limiting the time that the sample spends at the maximum sintering temperature. However, it does not solve the problem of sample porosity. Work is currently underway to examine the benefits of adding a calcination process to the sintering of bulk phase $BiFeO_3$.

References

1. Kimura, T. and Kawanoto, S., Magnetocapacitance in multiferroic $BiMnO_3$. *Phys. Rev. B*, 2003, **67**, 180401.
2. Pradham, A. K., Kai Zhang, D., Hunter, J., Dadson, B. and Loutts, G. B., Magnetic and electrical properties of single-phase multiferroic $BiFeO_3$. *J. Appl. Phys.*, 2005, **97**, 093903.
3. Kadomtseva, A. M., Zvezdin, A. K., Popov, Y. F., Pyatakov, A. P. and Vorob'ev, G. P., Space–time parity violation and magnetoelectric interactions in antiferromagnets. *JETP Lett.*, 2004, **79**, 571.
4. Wang, Y., Jiang, Q., He, H. and Nan, C., Multiferroic $BiFeO_3$ thin films prepared via a simple sol–gel method. *Appl. Phys. Lett.*, 2006, **88**, 142503.
5. Wang, Y. P., Zhou, L., Zhang, M. F., Chen, X. Y., Liu, J. M. and Liu, Z. G., Room-temperature saturated ferroelectric polarization in $BiFeO_3$ ceramics synthesized by rapid liquid phase sintering. *Appl. Phys. Lett.*, 2004, **84**, 1731.

6. Mahesh Kumar, M., Palkar, V. R., Srinivas, K. and Suryanarayana, S. V., Ferroelectricity in a pure $BiFeO_3$ ceramic. *Appl. Phys. Lett.*, 2000, **76**, 2764.
7. Zhang, S. T., Lu, M. H., Wu, D., Chen, Y. F. and Ming, N. B., Larger polarization and weak ferromagnetism in quenched $BiFeO_3$ ceramics with a distorted rhombohedral crystal structure. *Appl. Phys. Lett.*, 2005, **87**, 262907.
8. Hongri, L., Zuli, L., Qing, L. and Kailun, Y., Electric and magnetic properties of multiferroic $(BiFeO_3)_{1-x}$–$(PbTiO_3)_x$ films prepared by the sol–gel process. *J. Phys. D: Appl. Phys.*, 2006, **39**, 1022–1027.
9. Cheng, J.-R., Nan, L. and Eric Cross, L., Structural and dielectric properties of Ga-modified $BiFeO_3$–$PbTiO_3$ crystalline solutions. *J. Appl. Phys.*, 2003, **94**, 5153.
10. Mahesh Kumar, M., Srinivas, A. and Suryanarayana, S. V., Structure property relations in $BiFeO_3$/$BaTiO_3$ solid solutions. *J. Appl. Phys.*, 2000, **87**, 855.
11. Patterson, B. D., Abela, R., Auderset, H., Chen, Q., Fauth, F., Gozzo, F. *et al.*, The materials science beamline at the Swiss Light Source: design and realization. *Nucl. Instr. Methods Phys. Res. A*, 2005, **540**, 42–67.
12. Tang, C. C., Martin, C. M., Laundy, D., Thompson, S. P., Diakun, G. P. and Cernik, R. J., X-ray beam characteristics on MPW6.2 at the SRS. *Nucl. Instr. Methods Phys. Res. B*, 2004, **222**, 659–666.
13. Cernik, R. J., Barnes, P., Bushnell-Wye, G., Dent, A. J., Diakun, G. P., Flaherty, J. V. *et al.*, The new materials processing beamline at the SRS Daresbury, MPW6.2. *J. Synch. Rad.*, 2004, **11**, 163–170, Part 2.
14. Collins, S. P., Cernik, R. J., Fell, B., Tang, C. C., Harris, N. W., Miller, M. C. *et al.*, Station 16.3: a high-resolution single-crystal diffraction facility at the SRS, Daresbury. *J. Synch. Rad.*, 1998, **5**, 1263–1269.
15. Berry, A., Helsby, W. I., Parker, B. T., Hall, C. J., Buksh, P. A., Hill, A. *et al.*, The Rapid2 X-ray detection system. *Nucl. Instr. Methods Phys. Res. A*, 2003, **513**, 260–263.
16. Schmitt, B., Bronnimann, C., Eikenberry, E. F., Gozzo, F., Hormann, C., Horisberger, R. *et al.*, Mythen detector system. *Nucl. Instr. Methods Phys. Res. A*, 2003, **501**, 267–272.
17. Schmidt B, Private communication.
18. Modular Temperature Chambers for X-ray Diffraction User Manual, http://www.mri-gmbh.de/.
19. Cheary, R. W. and Coelho, A. A., A fundamental parameters approach of X-ray line-profile fitting. *J. Appl. Cryst.*, 1992, **25**, 109–121.
20. Kern, A. A. and Coelho, A. A., *A New Fundamental Parameters Approach in Profile Analysis of Powder Data*. Allied Publishers Ltd., 1998, pp. 144–51, ISBN: 81-7023-881-1.